Atomic Spectroscopy

Article

Temperature Difference Between Gas Species in Absorption Measurements Using Diode Laser Absorption Spectroscopy and Its Effect on Temperature Reduction

Akira Kuwahara, [a,*] Yasuaki Aiba,[b] Takuya Nankawa,[c] and Makoto Matsui [d]

[a] Department of Applied Energy, Nagoya University, Aichi 464-8603, Japan
[b] Department of Engineering, Shizuoka University, Shizuoka 432-8561, Japan
[c] Advanced Science Research Center, Japan Atomic Energy Agency, Ibaraki 319-1195, Japan
[d] Department of Mechanical Engineering, Shizuoka University, Shizuoka 432-8561, Japan

Received: *January 31, 2021;* ***Revised:*** *February 21, 2021;* ***Accepted:*** *February 21, 2021;* ***Available online:*** *February 22, 2021.*

DOI: 10.46770/AS.2021.006

ABSTRACT: The observation of isotope shifts due to a difference in mass number by diode laser absorption spectroscopy (DLAS) is a powerful approach for the isotope analysis of radionuclides. The spectral resolution for the detection of slight shifts can also be enhanced by a temperature reduction using adiabatic expansion. In our previous studies, we reported that the translational temperature was successfully decreased to approximately 180 K in xenon isotope analysis using a supersonic plasma jet. However, there remains a considerable uncertainty regarding the significant temperature reduction compared with the temperature of argon atoms at the edge of the supersonic plasma jet, which is at 790 K. In this study, temperature differences between two species of three mixed gas patterns (neon/argon, argon/strontium, and argon/xenon) were investigated using low-pressure glow discharge plasma. The temperature differences for the mixed gas patterns were clearly observed and are sufficient evidence to support our previous results. The relationship between temperature differences and energy levels of lower states used as absorption transitions is also discussed.

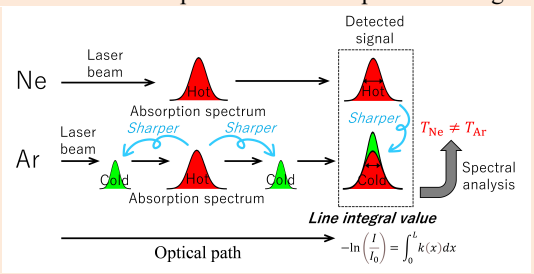

INTRODUCTION

Radioisotope abundance due to radioactive decay provides clues to its origin and age; thus, isotope analysis techniques are essential tools for obtaining accurate information.[1-4] In fact, radioactive elements (*e.g.* ^{90}Sr, ^{134}Cs, and ^{137}Cs) were released into the environment as a result of the accident at the Fukushima Daiichi Nuclear Power Plants in 2011,[5,6] and the quantification of their abundance is essential for the safe treatment and disposal of the contaminated radioactive waste.[7] Among them, ^{90}Sr (half-life of 30 years) is one of the most hazardous nuclides because it accumulates in biological bone and emits beta radiation (energy maximum of 0.54 MeV) to surrounding tissues over a long period of time. Strontium isotope analysis has been widely conducted by conventional measurement methods such as inductively coupled plasma mass spectrometry (ICP-MS) and liquid scintillation counting.[5,8]

ICP-MS, which is the most common isotope analysis method, characterizes isotopes by the mass difference of the elements. Thus, there is difficulty in measuring isotopes with the same mass, such as uranium (^{238}U) and plutonium (^{238}Pu), which are the major elements in nuclear waste, including in spent fuel.[9-11] In strontium analysis, ^{90}Y and ^{90}Zr, which are daughter and grandchild nuclides, respectively, considerably interfere with ^{90}Sr detection. To prevent technical issues during measurement, it is necessary to separate each element using chemical pretreatment, which usually is very time-consuming (approximately 2–4 weeks).[7] Therefore, the development of a measurement method with an easy sample pretreatment and achieves high accuracy essential for rapid analysis. Recently, highly sensitive optical spectroscopic methods for isotope analysis, such as absorption spectroscopy (diode laser

absorption spectroscopy (DLAS)) and fluorescence spectroscopy (laser-induced fluorescence (LIF)), have been developed.[12,13]

DLAS, which uses plasma as an atomization source, can characterize isotopes by a difference in the energy level of each element and the isotope shifts using diode lasers with high-wavelength selectivity; therefore, this approach has gained attention as a useful technique for isotope analysis. Because high resolution allows the detection of slight wavelength shifts, DLAS can distinguish isotopes with the same mass without any chemical pretreatment of the samples. However, the high-temperature condition of plasma observed with conventional instrumentation, which usually reaches 5000–10,000 K during laser ablation, decreases the spectral resolution as a result of the Doppler broadening because of thermal atomic motions.[14-20] For example, a 100-times increase in temperature usually causes a 1/10 decrease in resolution.[21]

In a previous study,[22] we proposed a rapid isotope analysis method without sample preparation by using a supersonic plasma jet. The arc discharge plasma in the high-temperature section upstream of a supersonic nozzle leads to a vacuum chamber; then, the translational temperature considerably decreases with an increase in the flow velocity because of adiabatic expansion. In a different study,[23] we used xenon gas as a target where a temperature reduction was successfully achieved and was estimated at approximately 180 K. However, in the above-mentioned study,[22] the temperature of the argon atoms at the edge of the plasma jet was determined to be 790 K. Thus, the results obtained with DLAS measurements suggested the possibility that the translational temperature of the xenon atoms differed from that of the argon atoms.

The present study aimed to investigate the temperature differences between two species by conducting temperature measurements using DLAS in a mixed gas plasma containing noble gases (neon, argon, and xenon) and strontium. As a plasma source, a low-pressure glow discharge plasma was used to generate a temporal and spatial steady-state plasma. A liquid phase sample, which contained a strontium compound, was supplied to an electrode before plasma generation. On the basis of the temperature differences obtained between the two species in glow discharge plasmas of the three mixed gas patterns, we discuss the relationship between the temperature differences and the energy levels of each atomic electron transition as well as the effect on the temperature reduction for the strontium atoms.

EXPERIMENTAL

Glow discharge plasma. A glow discharge plasma was produced between two cylindrical 20 mm diameter copper electrodes that were approximately 50 mm apart. The supply voltage can be adjusted between 0 and 3 kV with a high-voltage power supply (METRONIX: HSV2K-30). In the temperature measurements of the two species, two pinholes were positioned in front of each window because laser beams must pass through the same optical path in the glow discharge plasma. The operating conditions of the gas mixture were optimized to obtain temperatures for the two species simultaneously. An optical chopper (Thorlabs: MC200B), combined with a lock-in amplifier (Stanford Research Systems: SR830), was used to improve the signal-to-noise ratio.

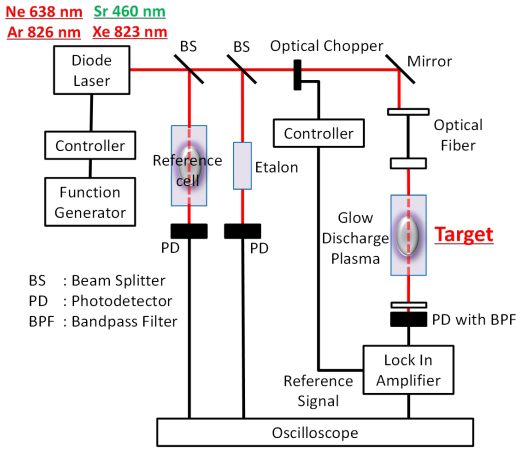

Fig. 1 Schematic diagram of the DLAS system using glow discharge plasma.

Diode laser absorption spectroscopic system. Fig. 1 shows the schematic diagram of the diode laser absorption spectroscopic system that uses a glow discharge plasma. DLAS analysis was performed using the single longitudinal mode diode lasers (Hitachi: HL6322G and HL8325G) which were tuned to the neon, argon, and xenon absorption lines. These laser line widths (approximately 100 MHz) were one order of magnitude narrower than the absorption line width (a few GHz) in the low-pressure glow discharge plasma. To detect strontium, an external cavity diode laser (Toptica: DL100) was used with the laser line width at approximately 100 kHz. Each laser wavelength was scanned over an absorption spectrum by modulating the laser operating current with a ramp function controlled with a low-cost function generator (A&D Company: AD-8624A). The repetition frequency was approximately 1 Hz and the scanning width approximately 10 GHz. The relative laser wavelength was observed using solid etalons (EKSMA: UVFS flat etalon finesse 30) with a free spectral range of 1.15 GHz for the 630 and 830 nm bands. An optical cavity consisting of two high-reflective mirrors (Sigmakoki Co., LTD.: PSCM95-25.4C6.35-1000-460) was installed in the free space for the 460 nm band. The transmitted laser beams through the plasma and the etalon were detected using a photodetector (Thorlabs: DET10/M). Their voltage signals were recorded using an oscilloscope (Yokogawa: DL850E) with a 12-bit resolution at the maximum sampling rate of 10 MS s^{-1}.

RESULTS AND DISCUSSION

To investigate the temperature differences in DLAS measurements, we generated glow discharge plasmas for the three mixed gas patterns (neon/argon, argon/strontium, and argon/xenon) and conducted the temperature measurements for two gases using each atomic absorption line. The wavelengths of neon, argon, strontium, and xenon in air were 638.30 nm (Ne I, $3s[3/2]^{O}_{1}$-$3p[3/2]_1$), 826.45 nm (Ar I, $4s[1/2]^{O}_{1}$-$4p[1/2]_1$), 460.73 nm (Sr I, $5s^2\ ^1S_0$-$5s5p\ ^1P^{O}_{1}$), and 823.16 nm (XeI, $6s[3/2]^{O}_{2}$-$6p[3/2]_2$), respectively.[24] The incident laser beam intensities that the plasmas were exposed to were set to sufficiently low power (<10 μW) to prevent absorption saturation.[25] To detect strontium, a $SrCl_2$ reagent sample (Fujifilm Wako Pure Chemical Co.: Strontium standard solution Sr 1000) was introduced into the electrode. Notably, only the strontium atoms were generated by the sputtering argon ions.

The absorption spectra of the neon, strontium, and xenon atoms comprised plural absorption lines because of the existence of isotopes, as shown in Fig. 2. In nature, neon, argon, strontium, and xenon have the following isotopes: three (^{20}Ne, ^{21}Ne, and ^{22}Ne), three (^{36}Ar, ^{38}Ar, and ^{40}Ar), four (^{84}Sr, ^{86}Sr, ^{87}Sr, and ^{88}Sr), and nine (^{124}Xe, ^{126}Xe, ^{128}Xe, ^{129}Xe, ^{130}Xe, ^{131}Xe, ^{132}Xe, ^{134}Xe, and ^{136}Xe), respectively. Under low-pressure conditions, the absorption profiles have an inhomogeneous broadening of the Doppler width, $\Delta\nu_D$, and these features can be expressed in Equations (1) and (2) as:[21]

$$f(\upsilon) = \frac{1}{\sqrt{\pi}\Delta\upsilon_D}\exp\left[-\left(\frac{\upsilon-\upsilon_0}{\Delta\upsilon_D}\right)^2\right] \quad \text{(Eq. 1)}$$

$$\Delta\upsilon_D = \frac{\upsilon_0}{c}\sqrt{\frac{2k_BT}{M_A}} \quad \text{(Eq. 2)}$$

where ν_0, M_A, and k_B are the center frequency, atomic weight, and Boltzmann constant, respectively. The neon, strontium, and xenon absorption spectra were treated with simplified convolutions of the Gaussian functions by considering each mass number, natural abundance, and oscillator strength.[26-28] Considering that the isotope abundance of ^{40}Ar is two orders of magnitude higher compared to other atoms, the absorption spectra of the argon atoms were fitted using a Gaussian function of the Igor Pro 6.2 software. The obtained absorption spectra agreed well with the fitting curves.

Fig. 3a-c shows the translational temperature measured at some discharge conditions of the three mixed gas patterns: (a) neon and argon, (b) argon and xenon), (c) argon and strontium. Remarkably, the temperature differences between the two species were clearly observed in the low-pressure glow discharge plasmas of these three patterns. The number densities of the strontium generated by ion bombardment increased approximately 46 times with an increase in the discharge current (Fig. 3c).

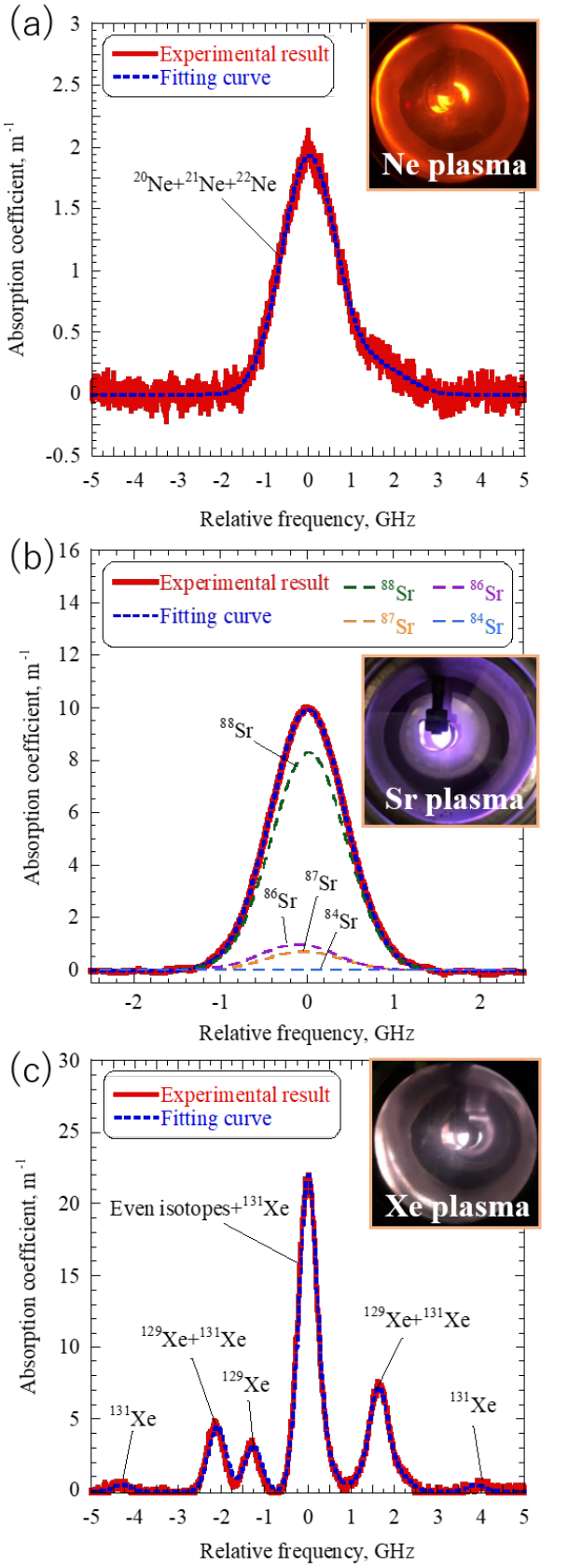

Fig. 2 Absorption profiles of (a) neon, (b) strontium, and (c) xenon atoms.

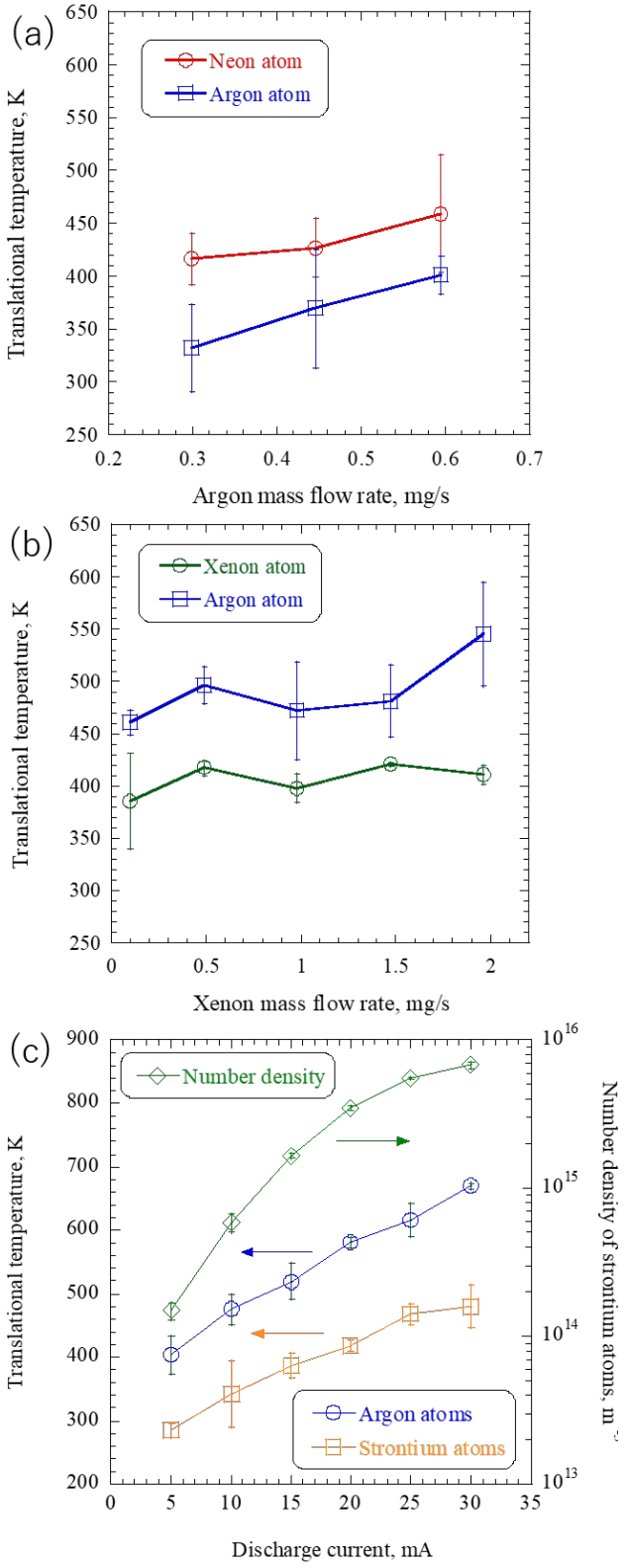

Fig. 3 Translational temperatures in mixed gas plasmas of three patterns. (a) Neon and argon atoms, (b) Argon and xenon atoms, (c) Argon and strontium atoms, and number densities of strontium atoms. Error bars represent standard deviations.

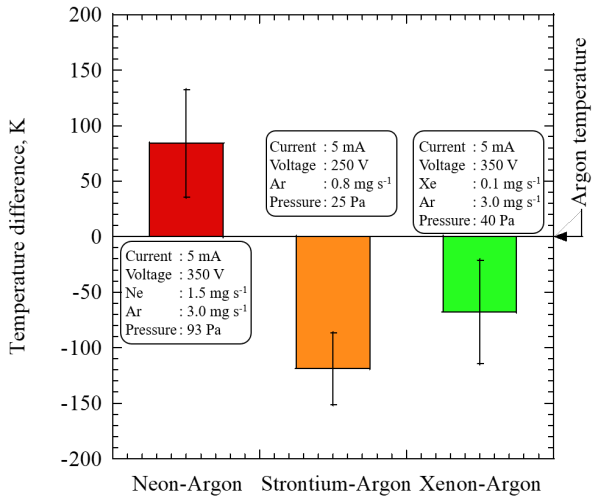

Fig. 4 Typical temperature differences in mixed gas plasmas of three patterns.

Fig. 4 shows the temperature differences between argon and the other atoms at each typical discharge condition. Indeed, similar to noble gases, these results showed that the temperature of the neon atoms was 84 K higher than for the argon atoms. Conversely, the temperature of the xenon atoms was 76 K lower than for the argon atoms. In the case of strontium detection, the temperature of the strontium atoms was 119 K lower than for the argon atoms.

This study attempts to identify the contributing factors for the temperature differences in DLAS measurements. Here, we discuss the relationship between the temperature measurements and the energy levels of the absorption transitions. DLAS has a feature where the obtained absorption spectrum is given by the line-integrated value over the optical path in the plasma because of tomography measurements. Considering that the absorption coefficient, $k(x)$, has a spatial distribution, the absorbance can be expressed in Equation (3) as:

$$-\ln\left(\frac{I}{I_0}\right) = \int_0^L k(x)dx \qquad \text{(Eq. 3)}$$

where I, I_0, and L are the transmitted beam intensity, incident beam intensity, and optical path length, respectively. Therefore, the temperature can be estimated as the average temperature of the optical path. If there is a difference in either the absorption coefficients or the optical paths, the temperatures obtained by fitting the integrated spectrum to the Gaussian function can also vary.

Figure 5 shows the relationship between the temperature differences and the energy levels of the absorption transitions, where the vertical axis indicates the energy level of a lower state in the absorption transition. In the present study, it was found that

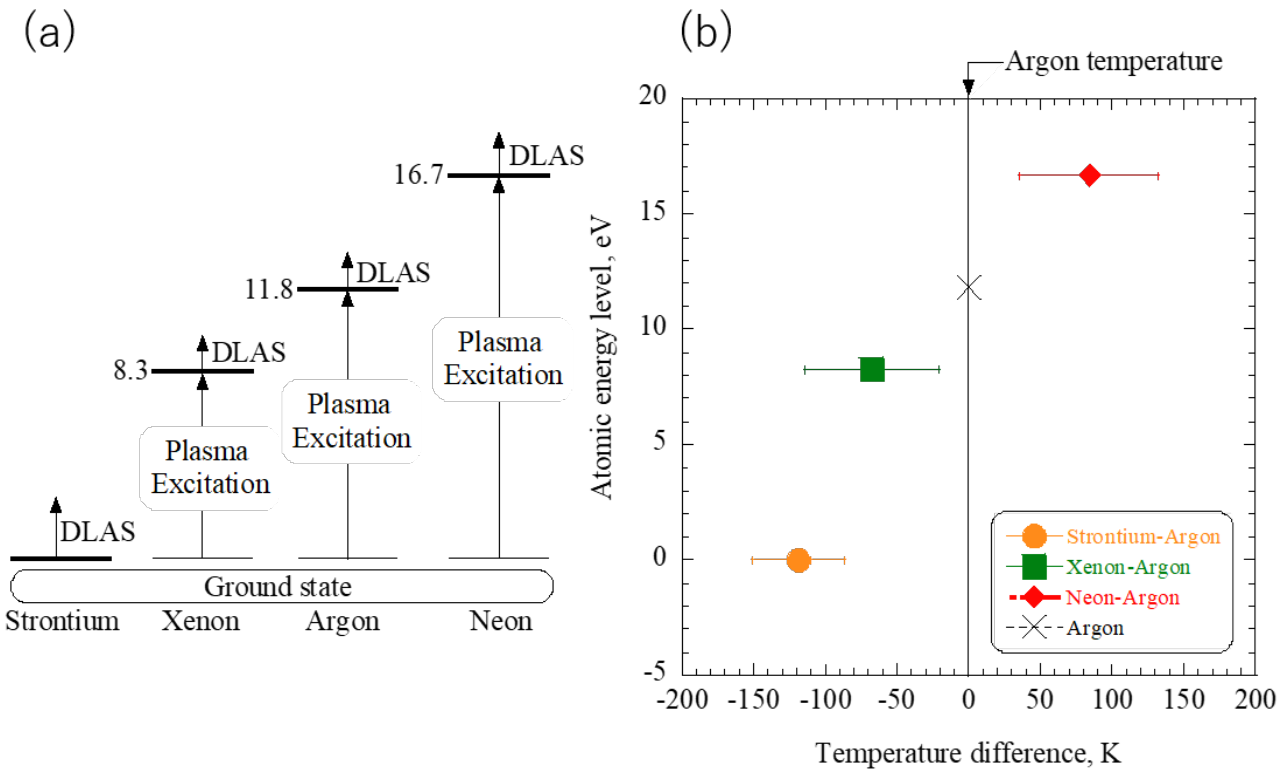

Fig. 5 Relationship between temperature difference and energy level of the lower state in absorption transition. (a) Experimental results of temperature differences. (b) Atomic energy level diagram of electron transitions. Error bars represent standard deviations.

the temperature differences were closely related to the energy levels, and the temperature decreased with a decrease in the energy level of the lower state. Most importantly, the energy levels of the excited states of the noble gases depend on the mass number.

Figure 6 shows the conceptual images of temperature difference. Fig. 6a assumes that the glow discharge plasma has a spatial temperature distribution.[29] Because atoms at a lower energy level are likely to be excited compared with those at a higher energy level, the temperature distribution due to the difference of normalized population distributions depends on the energy level.

It also can be seen that the population changes of the two energy states are negligible near the center of the temperature distribution (Fig. 6, area I), whereas the changes increase with a decrease in temperature (Fig. 6, area II). Hence, the temperature distribution is due to the difference in the population distributions of the two species. The contribution of atoms at the base (Fig. 6, area III) of the absorption spectra are negligible. In Fig. 6, area II, the gradient of the argon atoms is smaller than for the neon atoms, *i.e.*, the argon atoms are widely distributed in the plasma in comparison to the neon atoms.

The difference in population distribution can affect the absorption spectra in the temperature measurements by DLAS. Fig. 6b illustrates the absorption process by a probe laser beam in an optical path. Because the spatially detectable range of the argon atoms in an excited state extends to a lower temperature, the absorption spectrum (which is obtained as the line integral value over an optical path) sharpens; thus, the temperature can be estimated to be lower than for neon. Notably, there is a difference in the atomic behavior of ground and excited states because the atomic number density in the ground state is inversely proportional to the translational temperature according to the equation of the state. However, because the strontium atomization process depends on the sputtering of the argon ions in the glow discharge plasma, strontium atoms in the ground state are mostly distributed in the high-temperature area near the electrode.

In summary, the effect of temperature difference supports previous results regarding the temperature reduction for xenon atoms which is due to the lower energy levels of the argon and the xenon atoms. For strontium isotope analysis using the supersonic plasma jet system developed in our previous studies,[22,23] it will be more practical to sharpen an absorption spectrum of the strontium atoms, in addition to temperature reduction. Because of adiabatic expansion using a supersonic nozzle, the atoms in the ground state are expected to be distributed more near the edge of the supersonic plasma jet rather than near the center.[30] Additionally, because

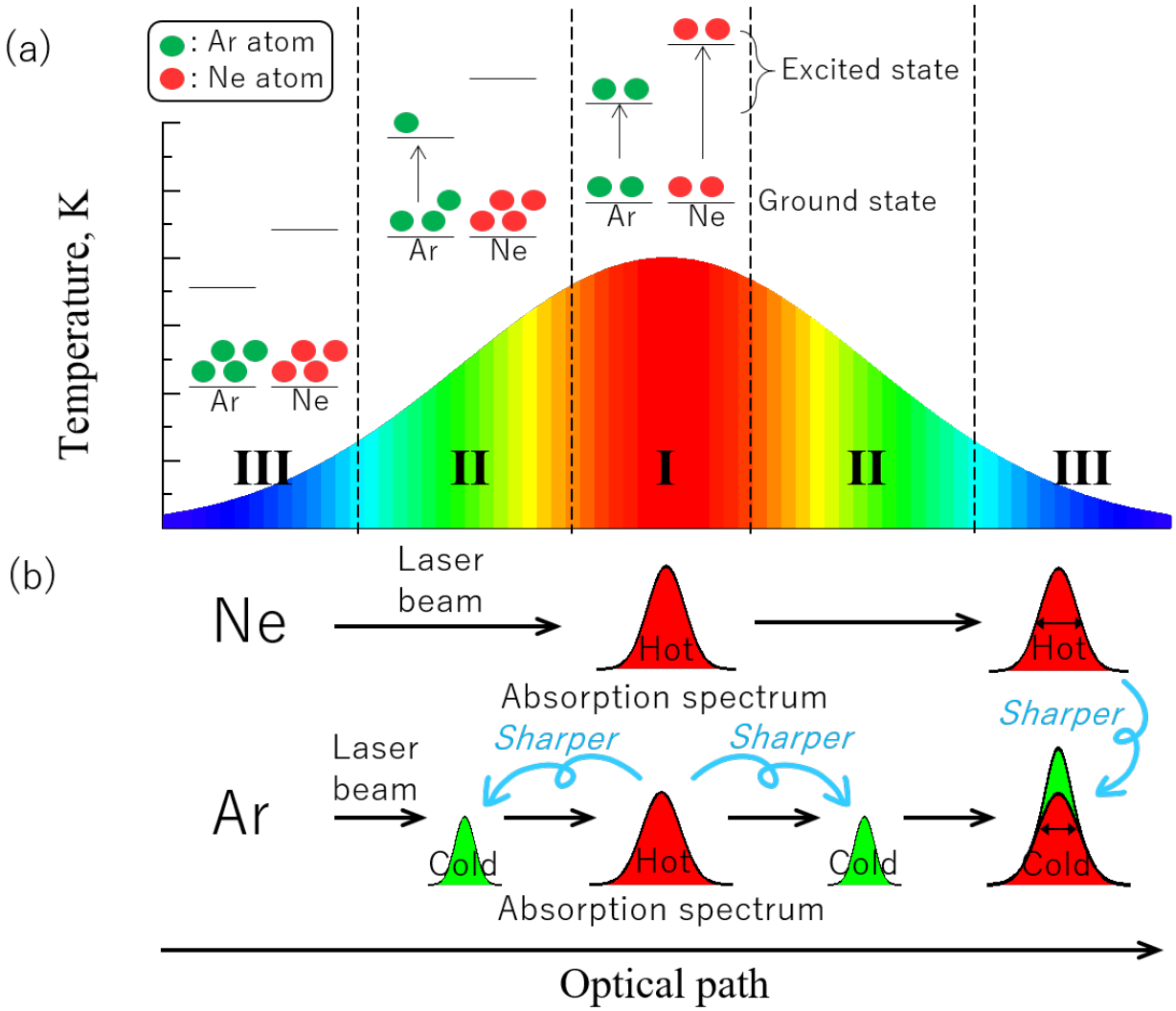

Fig. 6 Conceptual diagram of temperature difference due to the energy level in the absorption transition. (a) Spatial temperature and population distributions on the laser axis and an image illustrating atoms in an excited state. (b) Influence of temperature and population distribution on temperature measurements.

absorption transitions from the ground states in the isotope analysis of metallic elements can be used (*e.g.* Cs I, 852.1 nm; U I, 394.4 nm; and Pu I, 420.6 nm), significant temperature reductions can be expected for xenon atoms, in comparison to argon atoms.

CONCLUSIONS

The temperature measurements for two atomic electron transitions of different species revealed that there was an apparent temperature difference between the two species (list species). This phenomenon was attributed to the energy level differences in the lower states of absorption transitions. Thus, the present findings support our earlier study which showed that the translational temperature of the xenon atoms decreased considerably during xenon isotope analysis. The temperature measurements of the argon and strontium atoms indicate that the effect of temperature difference sharpened spectral broadening of the strontium atoms.

This study also showed that for strontium isotope analysis in a supersonic plasma jet, the temperature measurements for the argon and strontium atoms are still required. For temperature evaluations by DLAS without spatially resolved measurements, the effect of temperature difference should be analyzed by carefully considering the spatial population distribution in the case of an absorption transition from a relatively lower energy state, such as the ground state. Otherwise, the translational temperature will be underestimated.

AUTHOR INFORMATION

Corresponding Author

*A. Kuwahara

Email address: akuwahara@energy.nagoya-u.ac.jp

Notes

The authors declare no competing financial interest.

ACKNOWLEDGMENTS

This work was supported in part by JSPS KAKENHI Early-Career Scientists 18K14162 and the Environmental Research and Technology Development Fund 1RF-1702 of the Environmental Restoration and Conservation Agency of Japan.

REFERENCES

1. T. C. O'Connell and R. E. M. Hedges, *J. Archaeol. Sci*., 1999, **26**, 661–665. https://doi.org/10.1006/jasc.1998.0383
2. P. Szpak, D. R. Grocke, R. Debruyne, R. D.E. Macphee, R. D. Guthrie, D. Froese, G. D. Zazula, W. P. Patterson, and H. N. Poinar, *Palaeogeogr. Palaeoclimatol. Palaeoecol.*, 2010, **286**, 88-96. https://doi.org/10.1016/j.palaeo.2009.12.009
3. R. L. Malcolm, *Anal. Chim. Acta*, 1990, **232**, 19-30. https://doi.org/10.1016/S0003-2670(00)81222-2
4. Z. Varga, A. Nicholl, E. Hrnecek, M. Wallenius, and K. Mayer, *J. Radioanal. Nucl. Chem*., 2018, **318**, 1565-1571. https://doi.org/10.1007/s10967-018-6247-9
5. S. K. Sahoo, N. Kavasi, A. Sorimachi, H. Arae, S. Tokonami, J. W. Mietelski, E. Lokas, and S. Yoshida, *Sci. Rep.*, 2016, **6**, 23925. https://doi.org/10.1038/srep23925
6. T. Mizuno and H. Kubo, *Sci. Rep.*, 2015, **3**, 1742. https://doi.org/10.1038/srep01742
7. I. W. Croundace, B. C. Russell, and P. W. Warwick, *J. Anal. At. Spectrom.*, 2017, **32**, 494-526. https://doi.org/10.1039/C6JA00334F
8. N. Kavasi, S. K. Sahoo, A. Sorimachi, S. Tokonami, T. Aono, and S. Yoshida, *J. Radioanal. Nucl. Chem.*, 2015, **303**, 2565-2570. https://doi.org/10.1007/s10967-014-3649-1
9. J. S. Becker, *Spectrochim. Acta Part B*, 2003, **58**, 1757-1784. https://doi.org/10.1016/S0584-8547(03)00156-3
10. S. F. Boulyga and J. S. Becker, *J. Anal. At. Spectrom.*, 2002, **17**, 1143-1147. https://doi.org/10.1039/B202196J
11. C. G. Lee and S. H. Lim, *Nucl. Eng. Technol.*, 2018, **50**, 140-144. https://doi.org/10.1016/j.net.2017.10.010
12. A. Zybin, J. Koch, H.D. Wizemann, J. Franzke, and K. Niemax, *Spectrochim. Acta Part B*, 2005, **60**, 1-11. https://doi.org/10.1016/j.sab.2004.10.001
13. S. S. Harilala, B. E. Brumfield, N. L. LaHaye, K. C. Hartig, and M. C. Phillips, *Appl. Phys. Rev.*, 2018, **5**, 021301. https://doi.org/10.1063/1.5016053
14. A. Quentmeier, M. Bolshov, and K. Niemax, *Spectrochim. Acta Part B*, 2001, **56**, 45-55. https://doi.org/10.1016/S0584-8547(00)00289-5
15. H. Liu, A. Quentmeier, and K. Niemax, *Spectrochim. Acta Part B*, 2002, **57**, 1611-1623. https://doi.org/10.1016/S0584-8547(02)00105-2
16. M. Miyabe, M. Oba, H. Iimura, K. Akaoka, Y. Maruyama, and I. Wakaida, *Appl. Phys. A*, 2010, **101**, 65-70. https://doi.org/10.1007/s00339-010-5760-7
17. M. Miyabe, M. Oba, K. Jung, H. Iimura, K. Akaoka, M. Kato, H. Otobe, A. Khumaeni, and I. Wakaida, *Spectrochim. Acta Part B*, 2017, **134**, 42-51. https://doi.org/10.1016/j.sab.2017.05.008
18. M. C. Phillips, B. E. Brumfield, N. LaHaye, S. S. Harilal, K. C. Hartig, and I. Jovanovic, *Sci. Rep.*, 2017, **7**, 3784. https://doi.org/10.1038/s41598-017-03865-9
19. G. L. Donati and B. T. Jones, *J. Anal. At. Spectrom.*, 2011, **26**, 838-844. https://doi.org/10.1039/C0JA00172D
20. Y. Xiong, T. Lin, X. Jiang, X. Jiang, and X. Hou, *At. Spectrosc.*, 2020, **41**, 194-198. https://doi.org/10.46770/AS.2020.05.003
21. W. Demtroder, Laser Spectroscopy 1: Basic Principles, *Springer*, 2014.
22. A. Kuwahara, Y. Aiba, T. Nankawa, and M. Matsui, *J. Anal. At. Spectrom.*, 2018, **33**, 893-896. https://doi.org/10.1039/C8JA00040A
23. A. Kuwahara, Y. Aiba, Y. Yamasaki, T. Nankawa, and M. Matsui., *J. Anal. At. Spectrom.*, 2018, **33**, 1150-1153. https://doi.org/10.1039/C8JA00120K
24. National Institute of Standards and Technology, Atomic Spectra Database, NIST, Gaithersburg, MD, USA, 1997, https://www.nist.gov/pml/atomic-spectra-database.
25. M. Matsui, K. Komurasaki, S. Ogawa, and Y. Arakawa, *J. Appl. Phys.*, 2006, **100**, 063102. https://doi.org/10.1063/1.2353893
26. P. Jacquet and A. Pailloux, *J. Anal. At. Spectrom.*, 2013, **28**, 1298-1302. https://doi.org/10.1039/C3JA00010A
27. Y. Shimada, Y. Chida, N. Ohtsubo, T. Aoki, M. Takeuchi, T. Kuga, and Y. Torii, *Rev. Sci. Instrum.*, 2013, **84**, 063101. https://doi.org/10.1063/1.4808246
28. H. T. Do, H. Kersten, and R. Hippler, *New J. Phys.*, 2008, **10**, 053010. https://doi.org/10.1088/1367-2630/10/5/053010
29. V. P. Stepaniuk, T. Ioppolo, M. V. Otugen, and V. A. Sheverev, *J. Appl. Phys.*, 2007, **102**, 123302. https://doi.org/10.1063/1.2822338
30. M. Makoto, H. Takayanagi, Y. Oda, K. Komurasaki, and Y. Arakawa, *Vacuum*, 2003, **73**, 341-346. https://doi.org/10.1016/j.vacuum.2003.12.046